Available online at www.sciencedirect.com
SCIENCE DIRECT®
Polymer 45 (2004) 3729–3734
polymer
www.elsevier.com/locate/polymer

Statistical dynamic tensile strength of UHMWPE-fibers

Wen Huang, Yang Wang*, Yuanming Xia

Key Laboratory of Mechanical Behavior and Design of Materials, Department of Mechanics and Mechanical Engineering (5th), University of Science and Technology of China, Hefei, Anhui 230026, People's Republic of China

Received 24 November 2003; received in revised form 11 March 2004; accepted 12 March 2004

Abstract

Dynamic tensile properties of UHMWPE fiber bundles were studied at two strain rates and two temperatures. The integral stress–strain curves were obtained. Experimental data show that UHMWPE fiber bundle has strain rate and temperature sensitivity. A fiber-bundle constitutive equation was used to describe the tensile behavior of UHMWPE fiber bundles at high strain rates. The good consistency between the simulated results and experimental data indicates that the 5-parameter Weibull function can represent the tensile strength distribution of UHMWPE fibers and the method of extracting Weibull parameters from fiber bundles stress–strain data is valid.

Keywords: Fiber bundle; Tensile impact; Strength distribution

1. Introduction

Ultra highly oriented high molecular weight polyethylene—UHMWPE—fiber is increasingly used in bullet proof application, such as body armor and military helmets. It is an excellent reinforcement material for those weight-sensitive structures due to its high strength to weight ratio [1,2]. The ballistic resistance of fiber reinforced composite is essentially dependent on the mechanical behavior of the reinforcing component and the matrix. Fibers and fiber bundles carry the bulk of the applied load in a fiber-reinforced composite. The evaluation of its mechanical property thus requires the knowledge of the mechanical characteristics of the fibers. Especially, penetration and perforation process by high-speed projectiles is a dynamic and adiabatic process, where the transient adiabatic temperature rise occurs during the curse of impact loading. Consequently, the understanding of the strain rate and temperature sensitivity of the fibers is very important for the use and design of the fiber reinforced composites. Nevertheless, for UHMWPE fibers and fiber bundles, few experimental results on the strain rate and temperature effect on the mechanical properties have been reported.

It is well known that engineering fibers often exhibit a brittle fracture behavior and their tensile strength obey Weibull statistical distribution. Two experimental methods can be used to determine the strength statistical distribution parameters of fibers under quasi-static loading conditions. One is the single fiber test and the other is the fiber bundle test [3–10]. For single fiber testing method, it is rather tedious to extract individual fibers from a bundle and to perform numerous tests on fibers with very small diameter. The extraction of fibers from a bundle inevitably has 'select' the stronger ones, since the weaker fibers are prone to damage and fracture during handling prior to testing [4,9]. In contrast, a great number of fibers (usually hundreds or thousands) are included in a fiber bundle test, so it is possible to obtain the strength distribution characteristic of fibers with a relatively small number of tests. The fiber bundle testing method is increasingly used today. On the other hand, due to the technique difficulty, no suitable experimental technique is available to perform the dynamic single-fiber tension tests. Therefore, the fiber bundle testing method is the only choice for determining the dynamic tensile strength distribution of fibers under impact loading conditions [11–14].

The purpose of this paper is to study the effect of strain rate and temperature on the tensile mechanical properties of UHMWPE fiber bundles, and to evaluate the statistical distribution parameters of UHMWPE fibers by using dynamic fiber-bundle testing method.

* Corresponding author.
E-mail address: yangwang@ustc.edu.cn (Y. Wang).

0032-3861/$ - see front matter © 2004 Published by Elsevier Ltd.
doi:10.1016/j.polymer.2004.03.062

2. Tensile impact test

The dynamic tension tests were performed in the bar–bar tensile impact apparatus. An illustration of the setup and a Lagrangian X–T diagram which shows the details of the wave propagation in the bars are presented in Fig. 1. Through the impact of the hammer on the block, the prefixed short metal bar which is connected to the block and the input bar deforms and breaks. So an incident stress impulse is produced. Such stress impulse travels down the input bar and is partially reflected at the input bar/specimen interface and partially transmitted to the specimen and the output bar. The history of the incident strain $\varepsilon_i(t)$, reflected strain $\varepsilon_r(t)$ and transmitted strain $\varepsilon_t(t)$ are recorded at strain gages mounted on the input bar and output bars, respectively. Based on the one-dimensional wave propagation theory, the stress $\sigma_s(t)$, strain $\dot{\varepsilon}_s(t)$ and strain rate $\varepsilon_s(t)$ in the specimen can be calculated as follows:

$$\sigma_s(t) = \frac{E_b A_b}{2A_s}[\varepsilon_i(t) + \varepsilon_r(t) + \varepsilon_t(t)] = \frac{E_b A_b}{A_s}\varepsilon_t(t) \quad (1)$$

$$\varepsilon_s(t) = \frac{C_0}{l_s}\int_0^t [\varepsilon_i(\tau) - \varepsilon_r(\tau) - \varepsilon_t(\tau)]\mathrm{d}\tau = \frac{2C_0}{l_s}\int_0^t [\varepsilon_i(\tau) - \varepsilon_t(\tau)]\mathrm{d}\tau \quad (2)$$

$$\dot{\varepsilon}_s(t) = \frac{C_0}{l_s}[\varepsilon_i(t) - \varepsilon_r(t) - \varepsilon_t(t)] = \frac{2C_0}{l_s}[\varepsilon_i(\tau) - \varepsilon_t(\tau)] \quad (3)$$

where C_0 ($= \sqrt{E_b/\rho}$, E_b and ρ are the Young's modulus and density of the input/output bar, respectively) is the longitudinal wave velocity of the bar. A_b is the cross-sectional area of the input/output bar. A_s and l_s are the cross-sectional area and gage length of the specimen, respectively. The rise time and amplitude of the incident stress wave are determined by the impact velocity and the diameter of the prefixed short metal bar. So by varying the impact velocity and the diameter of the prefixed short metal bar, the tensile impact tests for any strain rate can be performed. The temperature chamber is placed between the input bar and output bar, which can be used to achieve the environmental temperature up to 120 °C.

The material investigated in the present study is UPMWPE fiber bundle (produced by DSM in Holland). A schematic diagram of the fiber bundle specimen and its connection with the input/output bars is shown in Fig. 2. The two lining blocks are glued to the supplement plate. The fiber bundles are wounded continuously onto each side of the lining blocks in parallel and uniform windings. Then the lining blocks with the bundles are bonded into the slots of the input/output bars using a high shear strength adhesive. The supplement plate is removed from the lining blocks before the tensile impact test. The specimen gage length is 8 mm.

The tensile impact tests were conducted at two high strain rates, 300/s and 700/s. The test temperature were 25 and 70 °C. Fig. 3(a)–(d) shows the integral tensile stress–strain curves under four test conditions, respectively. Each symbol type in the figure denotes a different specimen. It can be seen that the data coincide well with each other before the stress reaches the maximum value σ_b (failure stress). However, the data have a scatter after the strain greater than ε_b (unstable strain, corresponding to the failure stress). The possible sources of such data scatter for tensile impact test are related to winding of the fiber bundles onto the lining block and adhesive bonding of the fiber bundles to the lining blocks and the input/output bars. The uniform

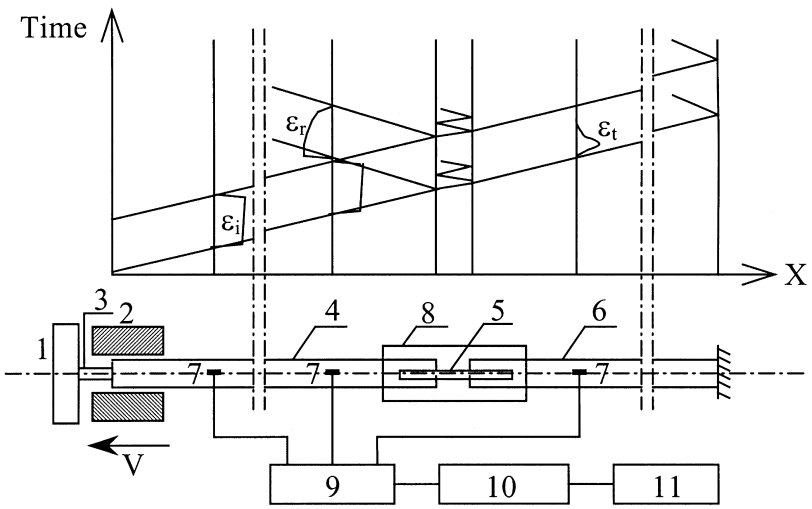

1- impact block 2- hammer 3- short prefixed metal bar 4- input bar 5- specimen
6- output bar 7- strain gage 8- temperature chamber 9- super dynamic amplifier
10- transient converter 11- computer

Fig. 1. Schematic diagram of bar–bar tensile impact apparatus and experimental principle.

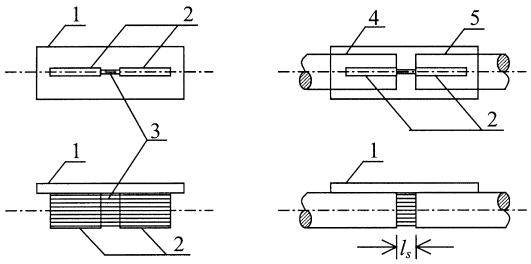

1- supplement plate 2- lining block 3- fiber bundles 4- input bar 5- output bar

Fig. 2. Fiber bundle specimen and its connection with input/output bars.

winding and reliable bonding are two critical procedures in the tests to avoid pullout phenomenon of the fiber bundles. Only the experimental stress–strain curves, which correspond to the tests without any fiber pullout, are shown in Fig. 3. The tensile properties of UHMWPE fiber bundles at different test conditions are listed in Table 1. It is seen that the initial Young's modulus decreases and unstable strain increases with increasing temperature at strain rate 300/s, respectively. Such phenomenon can also be seen at strain rate 700/s. The failure stress does not change apparently with the change of temperature and it decreases slightly when the temperature increases. In the case of strain rate sensitivity, the initial Young's modulus is relatively smaller at strain rate 300/s than that at 700/s at 25 °C, but it increases significantly at 70 °C when the strain rate increases. The unstable strain exhibits decrease trend with increasing strain rate and decreases significantly at 70 °C. However, the failure stress has no strain rate dependence and it is the same at strain rates 300/s and 700/s.

Table 1
Mechanical properties of UHMWPE fiber bundles

		E (Gpa)	σ_b (GPa)	ε_b (%)
300/s	25 °C	80	2.55	6.52
	70 °C	61	2.47	7.54
700/s	25 °C	82	2.55	6.26
	70 °C	68	2.48	6.57

3. Constitutive model

The stress–strain relation of fiber bundles subjected to

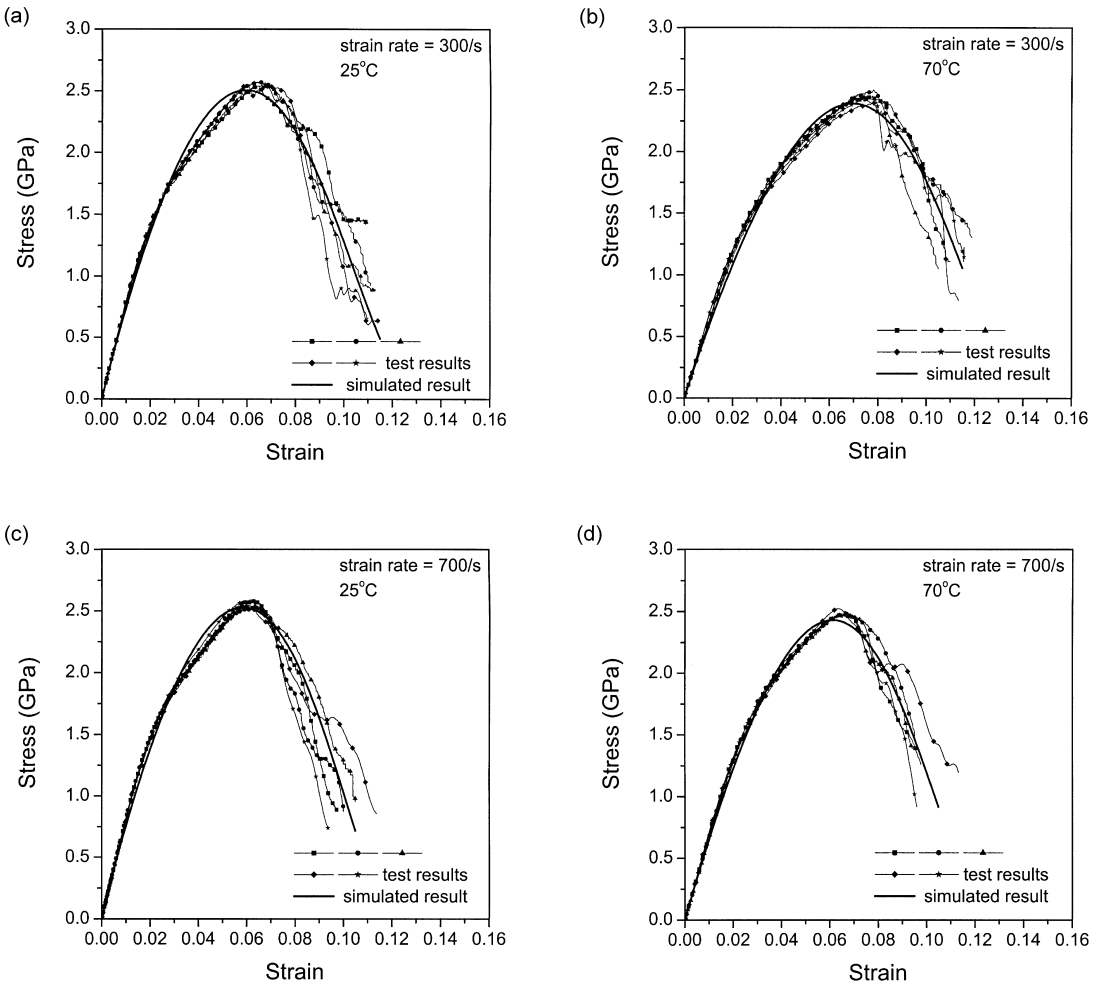

Fig. 3. Stress–strain curves of UHMWPE fiber bundles at different strain rates and temperatures.

dynamic tensile loading can be derived by using fiber bundle model which is composed of a large number of single fibers. The basic assumptions used in this model are presented as [11–16]:

(1) All fibers have the identical cross-sectional area and length.
(2) The lateral interaction of fibers is not taken into consideration.
(3) The applied tensile load is equally shared over the surviving fibers immediately when any fibers break.
(4) The tensile strength of fibers follows a particular statistical distribution. Usually, the two-parameter Weibull distribution expressed in Eq. (4) is adopted [17].

$$F(\sigma) = 1 - \exp\left[-\left(\frac{\sigma}{\sigma_0}\right)^m\right] \tag{4}$$

where $F(\sigma)$ is failure probability of single fiber under an applied stress no greater than σ at a certain constant strain rate. σ_0 and m are the scale and shape parameters of Weibull distribution function, respectively.
(5) For a single fiber, the stress–strain relation follows Hooke's law up to fracture at a certain constant strain rate.

Under these assumptions, the constitutive equation of fiber bundles under dynamic tensile loading conditions can be obtained. At an applied strain on the fiber bundles for a constant strain rate, the number of surviving fibers in the fiber bundles which initially have N_0 individual fibers is,

$$N_{\text{survial}} = N_0 \exp\left[-\left(\frac{E_f\varepsilon}{\sigma_0}\right)^m\right] = N_0 \exp\left[-\left(\frac{E\varepsilon}{\sigma_0}\right)^m\right] \tag{5}$$

E_f is Young's modulus of individual fiber and is equal to initial Young's modulus of fiber bundles, E, which can be experimentally evaluated from the stress–strain curve of fiber bundles.

This expression is then related to the applied tensile stress on the fiber bundles by

$$\sigma = \frac{T}{A_f N_0} = E\varepsilon \exp\left[-\left(\frac{E\varepsilon}{\sigma_0}\right)^m\right] \tag{6}$$

where T is the applied tensile load on the fiber bundles and A_f is the cross-sectional area of the single fiber. Eq. (6) is the constitutive equation of fiber bundles, which can describe the tensile behavior of fiber bundles.

The fiber strength distribution parameters are determined from the experimental stress–strain data of fiber bundles. For two-parameter Weibull distribution, σ_0 and m can be obtained via graphical method. Take double logarithms on the both side of Eq. (6), i.e.

$$\ln\left[-\ln\left(\frac{\sigma}{E\varepsilon}\right)\right] = m[\ln E\varepsilon - \ln \sigma_0] \tag{7}$$

The Weibull plot $\ln[-\ln(\frac{\sigma}{E\varepsilon})]$ against $\ln(E\varepsilon)$ will be straight line with the slope of the graph being equal to m.

Based on the experimental stress–strain data under a certain test conditions, the experimental Weibull curve $\ln[-\ln(\frac{\sigma}{E\varepsilon})]$ against $\ln(E\varepsilon)$ can be obtained. Fig. 4(a)–(d) shows the experimental Weibull curves at strain rates 300/s and 700/s and temperatures 25 and 70 °C, respectively. It should be emphasized that the experimental Weibull graph is not a straight line and exhibits a nonlinear characteristic. Obviously, it is too coarse to use a straight line to extrapolate this experimental Weibull curve. The two-parameter Weibull function is not appropriate for describing the strength statistical distribution of UHMWPE fibers, even though it has a simple form. Here a 5-parameter Weibull distribution function is introduced to incorporate such nonlinear characteristic [7]:

$$F(\sigma) = 1 - \exp\left[-\left(\frac{\sigma - \sigma_l}{\sigma_{01}}\right)^{m_1} / \left(\frac{\sigma_u - \sigma}{\sigma_{02}}\right)^{m_2}\right] \tag{8}$$

where σ_l and σ_u are the lower and upper strength limit. σ_{01}, σ_{02} and m_1, m_2 are the two scalar and shape parameters, respectively. Substituting Eq. (8) to (4), we have

$$\sigma = E\varepsilon \exp\left[-\left(\frac{E\varepsilon - \sigma_l}{\sigma_{01}}\right)^{m_1} / \left(\frac{\sigma_u - E\varepsilon}{\sigma_{02}}\right)^{m_2}\right] \tag{9}$$

For the fiber material which has preexisting defects in fibers and on fiber surfaces, it is reasonable to let the lower strength limit $\sigma_l = 0$ and the upper strength limit equal to some realistic theoretical maximum value [7]. Thus Eq. (9) can be reduced to

$$\sigma = E\varepsilon \exp\left[-\left(\frac{E\varepsilon}{\sigma_{01}}\right)^{m_1} / \left(\frac{\sigma_u - E\varepsilon}{\sigma_{02}}\right)^{m_2}\right] \tag{10}$$

An algorithm for nonlinear least square estimation of parameters is used to simulate the experimental points and estimate the five Weibull parameters, σ_u, σ_{01}, m_1, σ_{02} and m_2. The Weibull parameters at two strain rates and temperatures are listed in Table 2. The comparison of the stimulated stress–strain curves and Weibull curves with the experimental data is shown in Figs. 3 and 4, respectively. It can be seen that the simulated results agree well with experimental data, which confirms that the 5-parameter Weibull distribution function can represent the strength distribution of UHMWPE fibers subjected to high strain-rate loading.

Table 2
Weibull parameters estimated from fiber bundle tests

		σ_u (GPa)	σ_{10} (GPa)	m_1	σ_{02} (GPa)	m_2
300/s	25 °C	11.89	8.51	0.9	7.95	1.0
	70 °C	11.01	8.82	0.8	6.90	1.5
700/s	25 °C	11.03	8.41	0.9	6.58	0.9
	70 °C	10.90	7.99	1.0	7.01	1.3

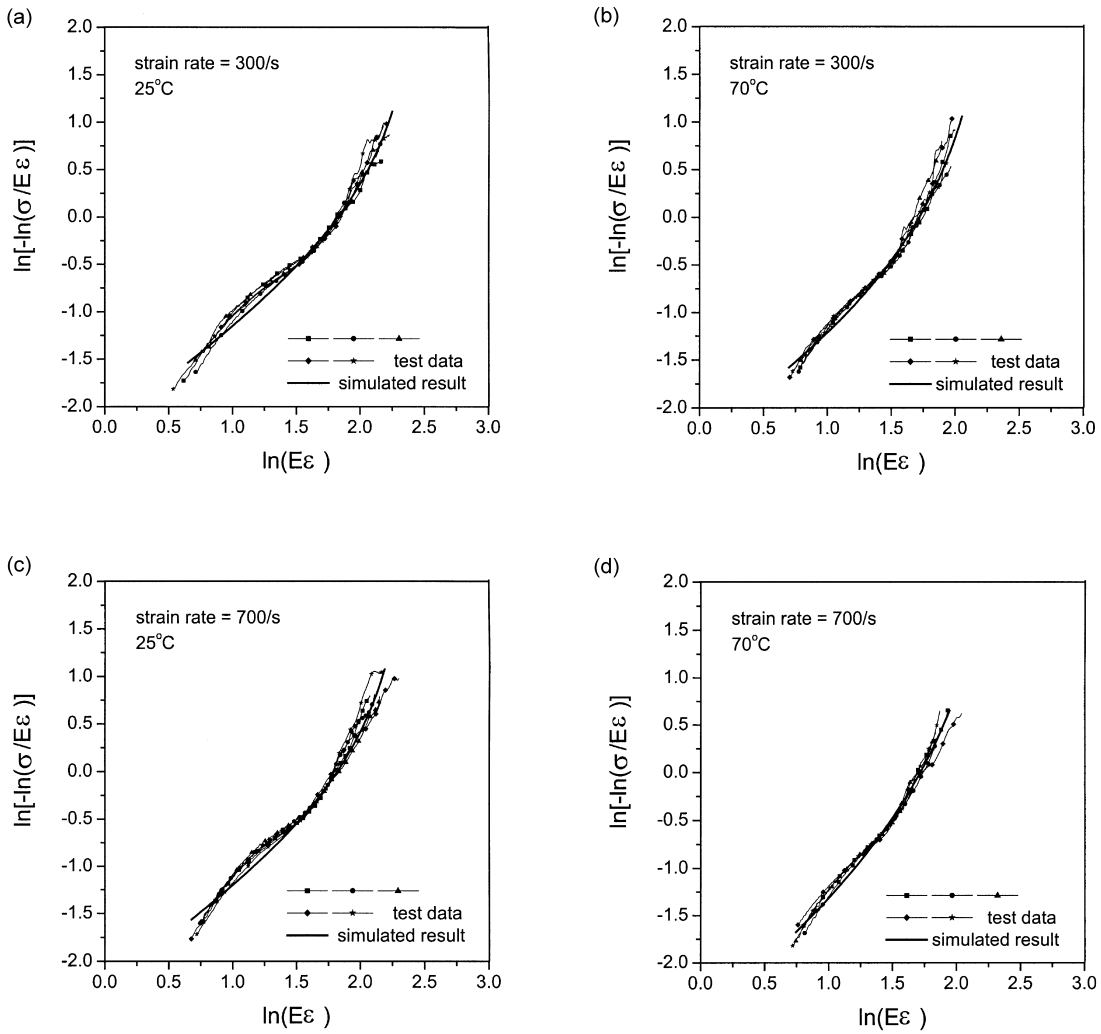

Fig. 4. Experimental Weibull curves and simulated results at different strain rates and temperatures.

4. Conclusion

(1) Tensile impact tests on UHMWPE fiber bundles were carried out at two strain rates and two temperatures. Experimental results show that the strain rate and temperature have some effect on the mechanical properties of HUMWPE fiber bundles. The Initial Young's modulus decreases significantly with the increase of temperature. The unstable strain increases with increasing temperature and decreases with increasing strain rate.

(2) The fiber bundle constitutive equation can integrally describe the tensile behavior of UHMWPE fiber bundles at high strain rates. It is appropriate to use the 5-parameter Weibull distribution function to characterize the strength distribution of UHMWPE fibers. The fiber bundle testing method is valid to derive the dynamic Weibull parameters from fiber bundle stress–strain data.

References

[1] Samara AZ, Harel H, Marom G, Yavin B. Polyethylene/polyethylene composite materials of ballistic protection. SAMPE J 1997;33(4): 72–5.

[2] Zee RH, Hsieh CY. Energy absorption processes in fibrous composites. Mater Sci Engng A 1998;246:161–8.

[3] Rosen BW. Tensile failure of fibrous composite. AIAA J 1964;2: 1985–91.

[4] Chi ZF, Chou TW, Shen GY. Determination of single fiber strength distribution from fiber bundle testings. J Mater Sci 1984; 19:3319–24.

[5] Watson AS, Smith RL. An examination of statistical theories for fibrous materials in the light of experimental data. J Mater Sci 1985; 20:3260–70.

[6] Goda K, Fukunaga H. The evaluation of the strength distribution of silicon carbide and alumina fibers by a multi-modal Weibull distribution. J Mater Sci 1986;21:4475–80.

[7] Phani KK. Evaluation of single-fiber strength distribution from fiber bundle strength. J Mater Sci 1988;23:941–5.

[8] Wilson DM. Statistical tensile strength of Nextel 610 and Nextel 720 fibers. J Mater Sci 1997;32:2535–42.

[9] Andersons J, Joffe R, Hojo M, Ochiai S. Glass fiber strength distribution determined by common experimental methods. Compos Sci Technol 2002;62:131–45.
[10] Standard test method for tensile strength and Young's modulus for high-modulus single-filament materials, ASTM D 3379–3375, 1989.
[11] Dong LM, Xia YM, Yang BC. Tensile impact testing of fiber bundles. Bangalore: ISCTAD Proc; 1990. p. 184–189.
[12] Xia YM, Yuan JM, Yang BC. A statistical model and experimental study of the strain-rate dependence of the strength of fibers. Compos Sci Technol 1994;52:499–504.
[13] Wang Z, Xia YM. Experimental evaluation of the strength of fibers under high strain rates by bimodal Weibull distribution. Compos Sci Technol 1997;57:1599–607.
[14] Wang Y, Xia YM. The effect of strain rate on the mechanical behavior of kevlar fiber bundles: an experimental and theoretical study. Compos Part A 1998;29A:1411–5.
[15] Daniels HE. The statistical theory of the strength of bundles of threads. Proc Roy Soc 1944/1945;A183:405–35.
[16] Coleman BD. On the strength of classical fiber and fiber bundles. J Mech Phys Solids 1958;7:60–70.
[17] Weibull W. A statistical theory of the strength of materials. Proc Roy Swedish Inst Engng Res 1939;151:1–45.